

Glass transition and crystallization of $0.8\text{TeO}_2 + 0.2\text{CdF}_2$ glass

D. Tatar^{a,*}, M.L. Öveçoğlu^a, G. Özen^b, B. Erim^b

^a Department of Metallurgical & Materials Engineering, Faculty of Chemical & Metallurgical Engineering,
Istanbul Technical University, Maslak 34469, Istanbul, Turkey

^b Department of Physics, Faculty of Science & Letters, Istanbul Technical University,
Maslak 34469, Istanbul, Turkey

Available online 10 June 2008

Abstract

The scope of this study is to determine the different crystal formation in the $0.8\text{TeO}_2 + 0.2\text{CdF}_2$ glasses heated with different rates to various annealing temperatures by using differential thermal analysis (DTA), X-ray diffraction (XRD) techniques, chemical analysis, optical microscope and scanning electron microscopy/energy dispersive spectroscopy (SEM/EDS). Different number of exothermic peaks were observed indicating the different crystallization or the transition of certain phases in the glass structure as the heating rate of DTA scans varied from 5 to $20^\circ\text{C}/\text{min}$. On the basis of the XRD investigations $\alpha\text{-TeO}_2$, $\gamma\text{-TeO}_2$ and CdTe_2O_5 crystalline phases were determined. SEM/EDS investigations of all the glasses revealed the presence of different phases correlated with the XRD analysis.

© 2008 Elsevier Ltd. All rights reserved.

Keywords: Tellurite glass; Microstructure; Thermal properties

1. Introduction

Tellurite glasses have more advantages over silicate and borate glasses because of their physical properties like low-melting temperature, high-refractive index, high-dielectric constant and good infrared transmissivity. Demonstrating a wide range of unique properties, tellurite glasses have potential applications such as pressure sensors, data storage, optical displays, optical amplifiers or as new laser hosts, optical modulators and optical memory storage systems.¹ Especially having the highest non-linear index n_2 in all possible oxide glasses, TeO_2 -based glasses with different components have become very prevalent which can be used as optical switches, second- and third-order non-linear optical materials.¹

TeO_2 structure does not form glass easily under normal quenching conditions but by adding other agents as glass modifiers, it is possible to make tellurite glasses.^{2,8,17} Typically tellurite glass network demonstrates paratellurite which is also known as $\alpha\text{-TeO}_2$ where TeO_4 units are only bonded at their corners. Further studies on the structure of the tellurite glasses have shown that there is the evidence of $\beta\text{-TeO}_2$, $\delta\text{-TeO}_2$ and lately found $\gamma\text{-TeO}_2$ phases in tellurite glass sys-

tems. $\gamma\text{-TeO}_2$ is formed in binary tellurite glasses heated slowly up to 440°C and annealed for 60 h.^{18,3,10,11} $\delta\text{-TeO}_2$ phase is expected to exist as a superposition of domains α -, β - and γ -crystalline phases that is also known as to be an intermediate phase between crystalline and glassy state and has a cubic structure.⁴

The potential use of the glass materials to design a fiber laser requires no crystallization in the matrix. Hence, it is vital to understand the crystallization behavior by studying the thermal properties and the microstructure for this application. This work includes the investigation of glass formation, thermal and the crystallization behavior of the $0.8\text{TeO}_2 + 0.2\text{CdF}_2$ binary glass. In literature a binary $\text{TeO}_2\text{--CdF}_2$ phase diagram does not exist but with the present investigation one of the possible glass forming compositions will be enlightened and studied which was found to be a non glass forming composition in earlier studies.^{2,5} The glass formation in the binary $\text{TeO}_2 + \text{CdF}_2$ system in literature takes place with CdF_2 contents varying between none to 0.15 mol.⁶ After the evaluation of the thermal properties with the help the differential thermal analysis (DTA) scans, the X-ray diffraction (XRD) and optical microscope and scanning electron microscopy/energy dispersive spectroscopy (Optical-SEM/EDS) characterizations of the glass were performed. Also chemical analyses of the samples were made with the atomic absorption technical to follow the compositional track.

* Corresponding author. Tel.: +90 212 285 3355; fax: +90 212 285 2925.
E-mail address: demettatar@yahoo.com (D. Tatar).

2. Experimental procedure

2.1. Glass synthesis

Glass synthesis was carried out by using high-purity TeO_2 (99.99% purity, Aldrich) and CdF_2 (99% purity, Aldrich) powders. Glass samples were prepared to constitute the composition of $0.8\text{TeO}_2 + 0.2\text{CdF}_2$ in molar ratio (now hereafter referred to as the $0.8\text{TeO}_2 + 0.2\text{CdF}_2$ glass). Power batches of 7 g were weighed in a PrecisaTM XB220A sensitive balance and ground in an agate mortar for 5 min. Glass melting was carried out using a Pt crucible with a closed lid in an electrically heated furnace at 900°C for about 60 min. The molten glass was removed from the furnace at 900°C and was cast by dipping the platinum crucible in a shallow water bath.

2.2. Thermal behavior and crystallization

DTA scans of as-cast $0.8\text{TeO}_2\text{--}0.2\text{CdF}_2$ glass specimens were carried out in TA Q 600 DTA DSC Instruments. The DTA scans were recorded using 3–15 g as-cast glass specimens which were powdered and heated with the heating rates of 5, 10 and $20^\circ\text{C}/\text{min}$ between 20 and 1000°C temperatures in a platinum crucible and using the same amount of alumina powder as the reference material. TA Instruments Universal Analysis Program was used to determine the glass transition temperatures (T_g), selected as the inflection point of the step change of the calorimetric signal and the peak temperatures (T_p) measured at the peak of crystallization. The effects of different heating rates on the crystallization T_p were also examined through the DTA curves with the heating rates of 5, 10 and $20^\circ\text{C}/\text{min}$. The heat-treated glass samples were prepared by heating the as-cast glasses above the crystallization peak temperatures obtained from the DTA analyses and quenched immediately by dipping the platinum crucible into water.

2.3. Microstructural characterization

Optical microscopy (OM) was performed with a NikonTM Eclipse L150 microscope equipped with NikonTM Coolpix 4.0 MP digital camera. SEM was carried out both in a JEOLTM Model JSM 5410 operated at 15 kV and linked with Noran 2100 Freedom energy dispersive spectrometer (EDS) attachment and in a JEOLTM Model JSM-T330 operated at 25 kV and linked with a Zmax 30 Boron-up light element EDS detector. For the OM and SEM investigations, optical mount specimens were prepared using standard metallographic techniques followed by chemical etching in a 95% distilled water + 5% HF solution for 10–20 s. The etched optical samples were coated

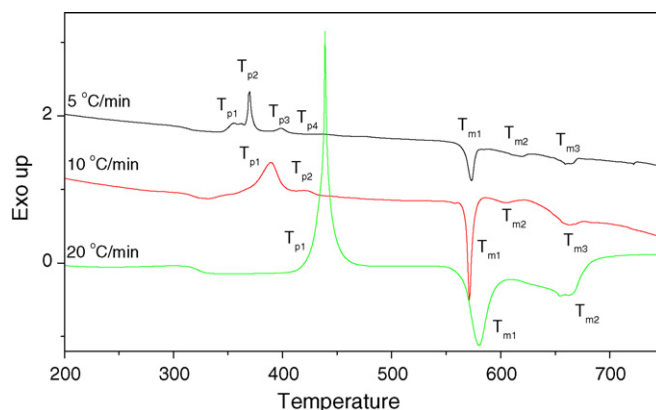


Fig. 1. DTA scans of the as-cast $0.8\text{TeO}_2\text{--}0.2\text{CdF}_2$ glass with different heating rates of 5, 10 and 20°C .

with palladium–gold for the SEM and SEM/EDS observations. XRD technique of the glasses scanned with the heating rates of 5, 10 and $20^\circ\text{C}/\text{min}$ glasses to certain annealing temperatures was performed using a Bruker D8 Advanced Series powder diffractometer and was used for acquiring the glass structure and the identification of the crystallized phases. All traces were recorded using $\text{Cu K}\alpha$ radiation at 1.5418 \AA and the diffractometer setting in the 2θ range from 10° to 90° by changing the 2θ with a step size of 0.02° . All samples were ground to fine powder for investigating and Eva Software was used to label peaks and then distinguish the crystalline phases existing in the sample. After obtaining the heat-treated glasses, The International Centre for Diffraction Data[®] (ICDD) data files were used for identifying the crystallized phases by comparing the intensities and the peak positions.

3. Results and discussion

3.1. DTA investigations

The DTA curves of as-cast glasses heated with different heating rates of 5, 10 and $20^\circ\text{C}/\text{min}$ are demonstrated in Fig. 1. Glass characterizing temperatures such as T_g , T_p and melting temperature (T_m) were also determined for each heating rate and are given in Table 1.

The curves exhibit an endothermic transition which corresponds to the glass transition temperature, T_g , and several exothermic peaks that give information about the crystallization or transformations of the crystalline phases.¹⁹ As it is known the beginning of the first exothermic reaction is the onset crystallization temperature where the crystallization first starts and the peak crystallization temperature is the maximum of the exotherm.⁶ Thermal investigations with DTA and DSC on different glasses

Table 1

Glass transition T_g , crystallization T_p , annealing T_a , melting T_m temperatures and the thermal stability K_g , of the glasses

B ($^\circ\text{C}/\text{min}$)	T_g	T_{p1}	T_{p2}	T_{p3}	T_{p4}	T_{a1}	T_{a2}	T_{a3}	T_{a4}	T_{m1}	T_{m2}	T_{m3}	K_g ($T_{p1} - T_g$)
5	314	356	369	399	440	365	383	411	457	574	620	660	42
10	315	389	423	–	–	400	450	–	–	572	605	662	74
20	320	439	–	–	–	475	–	–	–	580	–	660	119

have shown that increasing the heating rate also increases the related peak temperatures, and generally increases the peak areas with small amounts. As it can be seen from Fig. 1, the resolution between contiguous peaks change with different heating rates and demonstrates a range of thermal divergences, for that reason generally smaller heating rates are favored.²⁷ It can be observed from the DTA scans that with higher heating rates, peak temperatures gets higher and peak heights become larger. Both Fig. 1 and Table 1, also show that the glass transition temperature varies from 314 to 320 °C while the number of dominant crystallization peak temperatures decreases as the heating rate changes from 5 to 20 °C/min.

The difference between the first crystallization peak temperature (T_{p1}) and the T_g can be used to evaluate the glass forming tendency (K_g) which is a measure of the glass thermal stability.^{27,15} The thermal stability of a glass comprises the temperature interval during which the nucleation is occurring.²² Hurby parameter, K_{gl} , is also a unit revealing to the glass stability of the certain glass system and can be given as²⁶

$$K_{gl} = \frac{T_x - T_g}{T_m - T_x} \quad (1)$$

Both of the T_g and T_p temperatures increase from 314 to 320 °C and 365 to 431 °C, respectively, when the heating rate changes from 5 to 20 °C/min. As a result of these variations of T_g and T_p temperatures the glass-forming tendency also varies from 42 to 119 °C with the heating rate of the sample. On the literature, the glass-forming tendency of some ZnF_2 containing tellurium oxide glasses is reported to be greater than 160 °C which is greater than 119 °C obtained for the present glass system with 20 °C/min heating rate. However this values ($K_{gl} = 119$ °C) indicates that the $80TeO_2 + 20CdF_2$ binary glasses have higher thermal stability than some $TeO_2 + PbCl_2$ and $TeO_2 + K_2O$ glasses.^{5,16} The thermal stability of the $0.80TeO_2 + 0.20CdF_2$ binary glasses which has a value of 119 °C show similarity to the $0.90TeO_2 + 0.10BaO$ glass which is 123 °C.²¹

Different numbers of melting temperatures also exist for each scan. Glass heated with a 5 °C/min scanning rate exhibits three different endotherms at 574, 620 and 660 °C temperatures. Glass heated with a 10 °C/min exhibits three different endotherms at 572, 605 and 662 °C. Finally glass heated with a 20 °C/min scanning rate exhibits two different endotherms at 580 and 660 °C.

Four exothermic peaks at 356, 369, 399 and 440 °C following the glass transition at 314 °C are observed for the glass heated with a rate of 5 °C/min which indicates the existence of four different levels of crystallization or transformations of some phases in the glass matrix. Glass heated with 10 °C/min has demonstrated two exothermic reactions at 389 and 423 °C. Finally glass heated with 20 °C/min also demonstrates single exothermic peak at 439 °C. Since there are four different exothermic peaks on the thermal curves of the glass heated with the rate of 5 °C/m, there is only one peak on the curves of the glass heated with the rate of 20 °C/m. It can be claimed that the exothermic reactions taking place on the smaller heating rates, add up and appear as sums and overlaps which refers to the crystallization mechanism change. As a consequence it is harder to calculate the activation energy

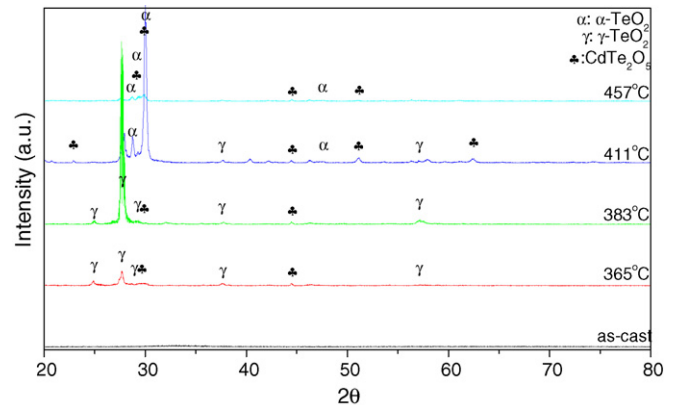


Fig. 2. XRD patterns of glasses heated to 365, 383, 411 and 457 °C temperatures with the heating rate of 5 °C/min.

and the Avrami parameter of the intersected exotherms and for that reason it is hard to indicate the crystallization mechanism of these glasses by using the non-isothermal technique. Having more than one exothermic peak refers to the existence of multiple phase of crystallization.^{13,20,22,24} Also with earlier studies it is understood that PbF_2 containing tellurite glass compositions show multiple crystallization peaks.^{2,9} At the same time there are PbF_2 containing tellurite glasses with single crystallization peaks as well.^{12,14}

3.2. XRD results

X-ray diffractometry scans were accomplished on the basis of DTA results to identify the crystallizing phases in the glasses annealed above the respective peak temperatures observed at different heating rates. The XRD pattern of as-cast glass was also recorded and given in Figs. 2–4. The spectrum exhibits a large amount of peak broadening at 2θ values ranging between 26° and 42° which indicates typical amorphous clustering of glassy solids.

Fig. 2 shows the X-ray diffraction patterns taken from the as-cast glass heated to 365, 383, 411 and 457 °C with the heating rate of 5 °C/min. As it can also be seen from the figure there are no detectable peaks in the as-cast glass. The glass

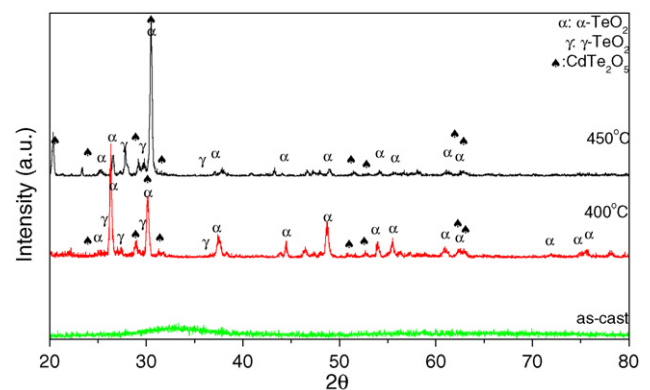


Fig. 3. XRD patterns of glasses heated to 400 and 450 °C temperatures with the heating rate of 10 °C/min.

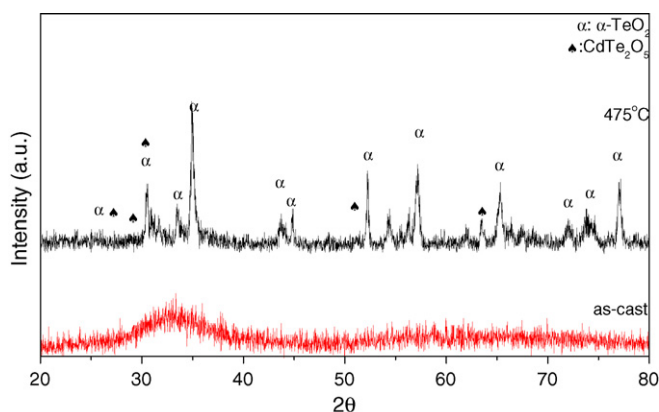


Fig. 4. XRD patterns of glasses heated to 475 °C with the heating rate of 20 °C/min.

heated to 365 °C with a heating rate of 5 °C/min shows γ -TeO₂ crystals with the addition of CdTe₂O₅ crystals in triclinic forms in its structure. As a following step in the glass heated to 383 °C, γ -TeO₂ crystals and the triclinic CdTe₂O₅ crystals exist with higher intensities. The glass heated to 411 °C has also γ -TeO₂ crystals but with less intensity relative to the glass heated to 383 °C on the other hand α -TeO₂ and CdTe₂O₅ crystalline phases form dominantly. When the glass was heated to 457 °C, the intensities of the α -TeO₂, CdTe₂O₅ and the γ -TeO₂ crystalline phases decrease as can be seen in Fig. 2. As a result, when the annealing temperature increases from 365 °C to 383 °C the metastable phase which is known as γ -TeO₂ is the dominant crystalline phase formed and when the temperature further increases to temperatures above 411 °C, the gamma phase diminishes and a new crystalline phase which is α -TeO₂ appears.^{28–30}

Fig. 3 shows the X-ray diffraction patterns taken from the as-cast glass heated to 400 and 450 °C temperatures with the heating rate of 10 °C/min. Glass heated to 400 °C demonstrates dominantly α -TeO₂ (paratellurite) and some Cd₂TeO₅ crystals and also very little amount of γ -TeO₂ in its structure. Despite the lower heating rate of 5 °C/min the crystal structure of the Cd₂TeO₅ formation in the glass heated with 10 °C/min is monoclinic. As further step heating the glass to a higher temperature of 450 °C results in the formation of dominantly monoclinic CdTe₂O₅ crystals and some paratellurite and little amount of γ -TeO₂ crystals in the glass matrix. As it can be seen from the XRD scan some of the crystalline phases in the glass structure formed in intermediate annealing temperatures decomposed and diminished in the final XRD pattern. The transformation of γ -TeO₂ to α -TeO₂ takes place in this heating rate as well because even though one of the initial crystals formed in the first annealing

step was γ -TeO₂, it diminishes mostly in the last step of heating and α -TeO₂ crystals take their place.

Fig. 4 shows the X-ray diffraction pattern taken from the as-cast glass heated to 475 °C with the heating rate of 20 °C/min. As it can be seen from the DTA scans the 0.8TeO₂–0.2CdF₂ glass has one exothermic peak at 439 °C. Glass heated to 475 °C has dominantly α -TeO₂ crystalline phase in its structure with the addition of monoclinic CdTe₂O₅.

Regardless the heating rate two dominant crystalline phases formed are α -TeO₂ and CdTe₂O₅ phases in the 0.8TeO₂–0.2CdF₂ binary glass composition. Triclinic CdTe₂O₅ phase is observed in lower heating rate while the CdTe₂O₅ formation occurred in monoclinic type for higher heating rates. As it can be seen from the XRD patterns given in Figs. 2–4 that the CdTe₂O₅ which is also known as cadmium ditellurite is one of the ferroelastic ditellurites.^{23,15,25} CdTe₂O₅ crystals have two different crystal structures as triclinic and monoclinic. It was studied by Redman and detected as mica like and piezo-electric. Crystal structures, lattice parameters, space group and card numbers of the crystal phases that are formed in the glasses are given in Table 2.

3.3. SEM and SEM/EDS Investigations

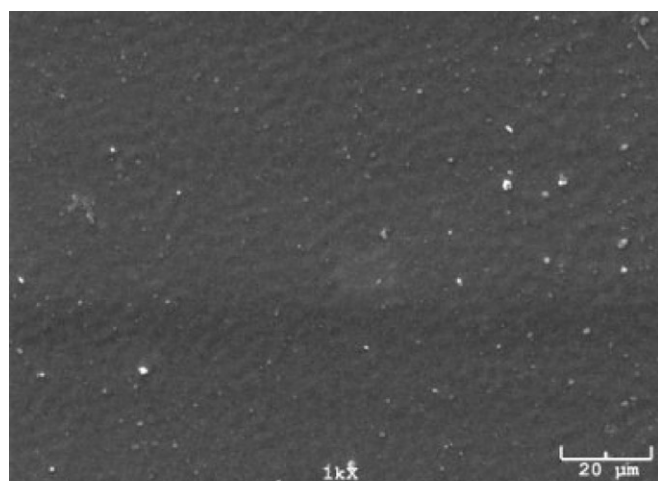
Fig. 5(a)–(c) shows the morphology of the crystalline phase formed when the glass is annealed at 383, 411 and 457 °C with the heating rate of 5 °C/min. The crystal sizes at 383 °C annealing temperature might be very small since the microstructure of the glass looks like amorphous with small grains even though it contains some crystalline phase. According to its XRD pattern the dominant crystalline phase was γ -TeO₂ (see Fig. 2) hence the morphology observed in the SEM image must be due to the formation of the gamma crystalline phase.

Fig. 5(b) shows the morphology of the glass structure formed when the sample was annealed at 411 °C. As the α -TeO₂ and CdTe₂O₅ crystal formations occur in the glassy matrix as it can be identified from the XRD pattern for the glass annealed at 411 °C, the microstructure of the glass changes and the number and the sizes of the grains become larger which indicates the increment of the volume fraction of the crystalline phase with respect to that of the glass phase. Fig. 5(c) represents the morphology of the glass structure formed when the sample was annealed at 457 °C. It is mainly formed by the glassy phase which is consistent with the relative intensities of the crystalline phases observed in their XRD patterns.

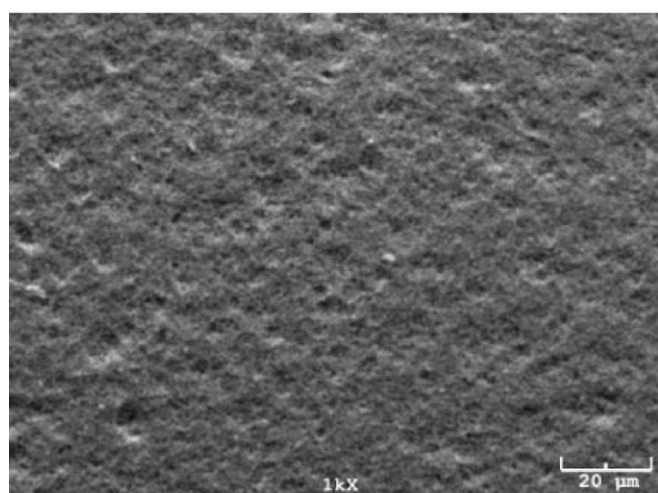
Fig. 6(a) represents the microstructure of the 0.8TeO₂–0.2CdF₂ glass heated with a rate of 10 °C/min to 400 °C which is above the first peak crystallization temper-

Table 2
Crystal structure, lattice parameters, space group, figure numbers and the card numbers of the crystallized phases

Crystal	Crystal structure	Space group	<i>a</i> (nm)	<i>b</i> (nm)	<i>c</i> (nm)	α (°)	β (°)	γ (°)	CN	Reference
α -TeO ₂	Tetragonal	<i>P</i> 4 ₁ 2 ₁ 2(92)	4.81011		7.6122	90	90	90	42-1365	1, 5
γ -TeO ₂	Orthorhombic	<i>P</i> ***(0)	8.448	4.993	4.2995	90	90	90	52-0795	1, 10
CdTe ₂ O ₅	Monoclinic	<i>P</i> 2/ <i>m</i> (10)	6.81	3.84	9.85	90	115.2	90	49-1755	15
CdTe ₂ O ₅	Triclinic	<i>P</i> -1(2)	6.866	3.801	9.098	100.67	85.44	89.25	36-0345	15



(a)



(b)

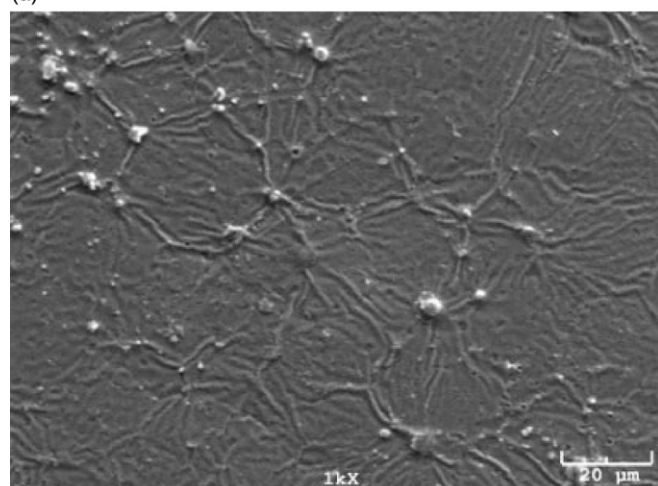


(c)

Fig. 5. Glasses heated with a scanning rate of 5 °C/min to 383, 411 and 457 °C: (a) SEM micrograph of glass surface annealed at 383 °C; (b) SEM micrograph of glass surface annealed at 411 °C; (c) OM micrograph of glass cross-section annealed at 457 °C.



(a)

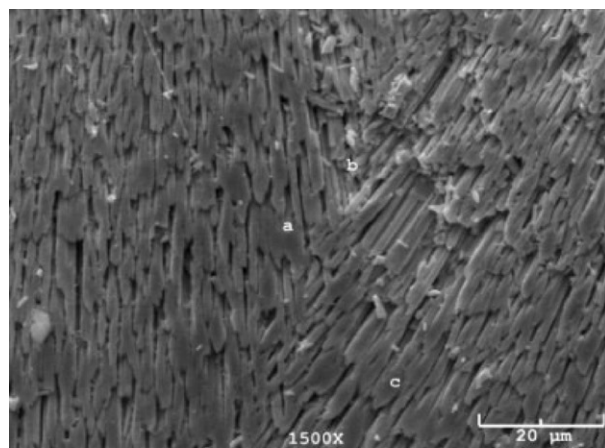


(b)

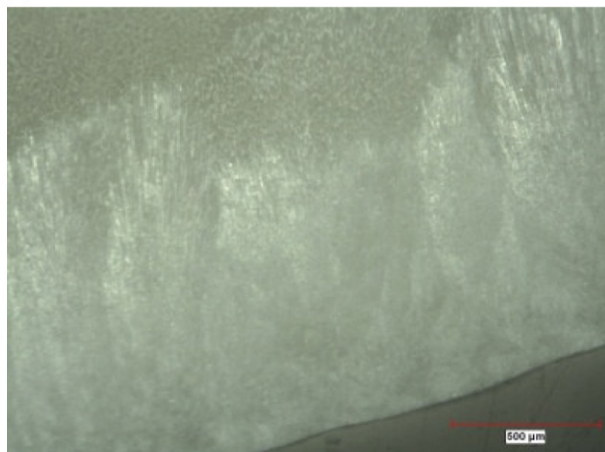
Fig. 6. Glasses heated with a scanning rate of 10 °C/min to 400 and 450 °C: (a) OM micrograph of glass cross-section annealed at 400 °C; (b) SEM micrograph of glass surface annealed at 450 °C.

ature observed in its DTA curve. XRD pattern given in Fig. 3 demonstrates the crystal formation of α -TeO₂, γ -TeO₂ and monoclinic CdTe₂O₅ phases in the glass structure. Optical micrograph of the glass shows a better representation of the glass morphology and structure. Fig. 6(b) represents the glass heated to 450 °C. It demonstrates very little amount of γ -TeO₂, α -TeO₂ and also monoclinic CdTe₂O₅ crystals relatively to the glass annealed at 400 °C with stronger intensities. It can be seen that the grains given in Fig. 6(b) transforms in to the dendrite like structures.

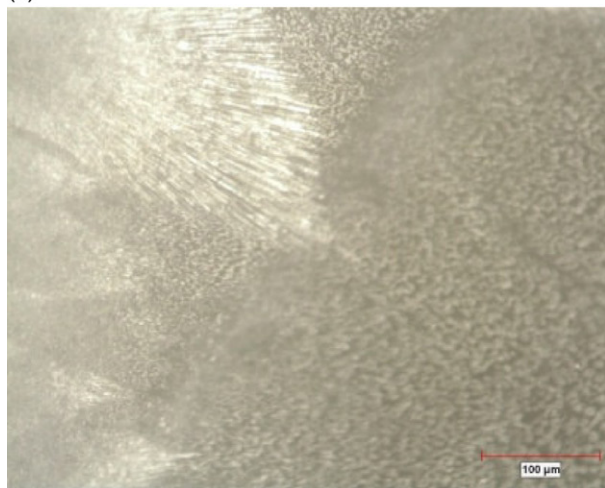
The microstructure of the 0.8TeO₂ + 0.2CdF₂ glass heated with a rate of 20 °C/min to 475 °C are represented in Fig. 7(a)–(f). XRD pattern given in Fig. 7 demonstrates formation of α -TeO₂ and monoclinic CdTe₂O₅ crystals. As it can be seen from the figures, the major portion of the glass matrix was crystallized. In Fig. 7(a) dendrites are clearly visible and demonstrates the crystallization of α -TeO₂ phase. EDS spectra taken from the rectangular/square-shaped dendrites (labeled by a, b and c in Fig. 7(a) and (d)) revealed that these grains contained 28.010 ± 0.8 wt.% Te, 0.194 ± 0.4 wt.% Cd and 71.613 ± 0.5 wt.% O, indicating the fact they belong to the



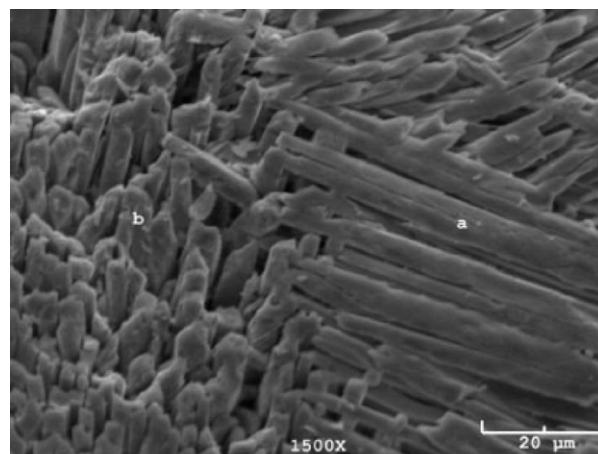
(a)



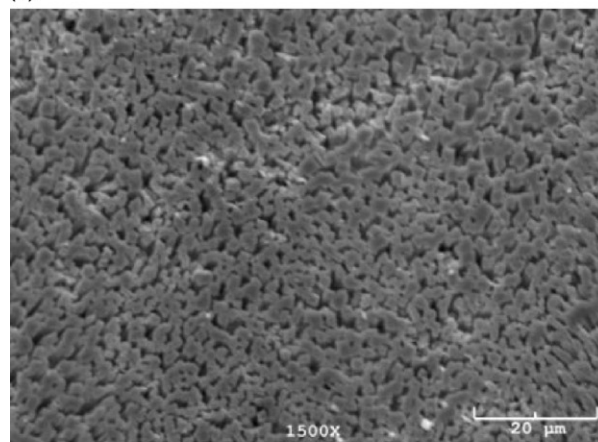
(b)



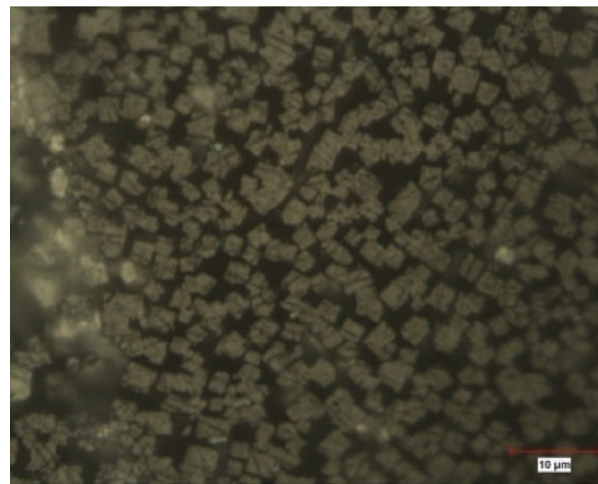
(c)



(d)



(e)



(f)

Fig. 7. Glasses heated with a scanning rate of 20 °C/min to 475 °C: (a) SEM micrograph of glass surface annealed at 475 °C; (b) OM micrograph of cross-section annealed at 475 °C; (c) OM micrograph of surface annealed at 475 °C; (d) SEM micrograph of cross-section annealed at 475 °C; (e) SEM micrograph of cross-section annealed at 475 °C; (f) OM micrograph of cross-section annealed at 475 °C.

Fig. 7. (Continued)

α -TeO₂ crystalline phase also detected in the XRD scan (Fig. 4). The size of the dendrites is founded be about 2–3 μm in width and they grow in different directions as it can be seen in Fig. 7(d).

4. Conclusions

The glass formation of 80TeO₂ + 20CdF₂ composition was achieved during this study which was not reported in the lit-

erature and found to be out of the glass forming region for the $\text{TeO}_2\text{--CdF}_2\text{--PbF}_2$ ternary glass system.⁶ Glass transition, peak crystallization temperature and the melting temperatures are found to be varying with the heating rate. Variations of the values of T_g and T_p temperatures cause a change in the glass forming tendency from 42 to 119 °C with the heating rate of the sample varying from 5 to 20 °C/min. Crystal formation of $\alpha\text{-TeO}_2$ and $\gamma\text{-TeO}_2$ with the addition of both monoclinic and triclinic CdTe_2O_5 crystal phases were observed when the glass samples were annealed to temperatures above the crystallization temperatures. While there are four different exothermic peaks on the thermal curves of the glass heated with rate of 5 °C/min, there is only one peak on the curves of the glass heated with rate of 20 °C/min. It can be claimed that the exothermic reactions taking place on the smaller heating rates, add up and appear as sums and overlaps which refers to the change of the crystallization mechanism.

Acknowledgements

The authors of this study express their gratitude to Dr. Nuri Solak for his comments on the XRD and DTA analysis. This research has been supported by the Scientific and Research Council of Turkey (TÜBİTAK) for the financial support under the project numbered 106T347.

References

1. El-Mallawany, A. H., *Tellurite Glasses Handbook*. CRS Press, London, 2002.
2. Kabalcı, İ., Özen, G., Öveçoğlu, M. L. and Sennaroğlu, A., Thermal study and linear optical properties of $(1-x)\text{TeO}_2\text{--}(x)\text{PbF}_2$ ($x=0.10, 0.15$ and 0.25 mol) glasses. *J. Alloys Compd.*, 2006, **419**, 294–298.
3. Mirgorodsky, A. P., Merle-Mejean, T., Champarnaud, J.-C., Thomas, P. and Frit, B., Dynamics of structure of TeO_2 polymorphs: model treatment of paratellurite and tellurite; Raman scattering evidence for new γ - and δ -phases. *J. Phys. Chem.*, 2000, **61**, 501–509.
4. Blanchandin, S., Marchet, P., Thomas, P., Champarnaud-Mesjard, J. C. and Frit, B., New investigations within the $\text{TeO}_2\text{--WO}_3$ system: phase equilibrium diagram and glass crystallization. *J. Mater. Sci.*, 1999, **34**, 4285–4292.
5. Öz, B., Kabalcı, İ., Öveçoğlu, M. L. and Özen, G., Thermal properties and crystallization behavior of some $\text{TeO}_2\text{--K}_2\text{O}$ glasses. *J. Eur. Ceram. Soc.*, 2007, **27**, 1823–1827.
6. Silva, M. A. P., Briois, V., Poulain, M., Messaddeq, Y. and Ribeiro, S. J. L., Lead–cadmium oxyfluoride glasses and glass–ceramics. *J. Phys. Chem. Solids*, 2002, **4**(3), 799–808.
8. Villegas, M. A. and Fernandez Navaro, J. M., Physical and structural properties of glasses in the $\text{TeO}_2\text{--TiO}_2\text{--Nb}_2\text{O}_5$ system. *J. Optoelectron. Adv. Mater.*, 2007, **27**, 2715–2723.
9. Öveçoğlu, M. L., Kabalcı, İ., Özen, G. and Öz, B., Microstructural characterization of $(1-x)\text{TeO}_2\text{--}x\text{PbF}_2$ ($x=0.10$ and 0.25 mol) glasses. *J. Eur. Ceram. Soc.*, 2007, **27**, 1801–1804.
10. Champarnaud-Mesjard, J. C., Blanchandin, S., Thomas, P. and Mirgorodsky, A., Crystal structure, Raman spectrum and lattice dynamics of a new metastable form of tellurium dioxide: $\gamma\text{-TeO}_2$. *J. Phys. Chem. Solids*, 2000, **61**, 1499–1507.
11. Dewan, N., Sreenivas, K. and Gupta, V., Properties of crystalline $\gamma\text{-TeO}_2$ thin film. *J. Cryst. Growth*, 2007, **305**(1), 237–241.
12. Bueno, L. A., Messaddeq, Y., Dias Filho, F. A. and Ribeiro, S. J. L., Study of fluorine losses in oxyfluoride glasses. *J. Non-Cryst. Solids*, 2005, **351**, 3804–3808.
13. Yukimitu, K., Oliveria, R. C., Araujo, E. B., Moraes, J. C. S. and Avanci, L. H., DSC studies on crystallization mechanisms of tellurite glasses. *Thermochim. Acta*, 2005, **426**, 157–161.
14. Poulain, M. and Poulain, M., Multicomponent fluoride glasses. *J. Non-Cryst. Solids*, 1997, **213**, 40–43.
15. Robertson, D. S., Shaw, N. and Young, I. M., A study of crystals in the cadmium oxide–tellurium dioxide system. *J. Mater. Sci.*, 1978, **13**, 1986–1990.
16. Wang, G., Dai, S., Zhang, J., Wen, L., Yang, J. and Jiang, Z., Thermal, optical properties and structural investigation of $\text{TeO}_2\text{--PbCl}_2$ glassy system. *J. Phys. Chem. Solids*, 2005, 1–5.
17. Akagi, R., Handa, K., Ohtori, N., Hannon, A. C., Tatsumisago, M. and Umesaki, N., High-temperature structure of $\text{K}_2\text{O--TeO}_2$ glasses. *J. Non-Cryst. Solids*, 1999, **256–257**, 111–118.
18. O'Donnell, M., *Tellurite and Fluorotellurite Glasses for Active and Passive Fibreoptic Waveguides*. PhD Thesis, The University of Nottingham, UK, 2004.
19. Cenk, S., Demirata, B., Öveçoğlu, M. L. and Özen, G., Thermal properties and optical transition probabilities of Tm^{3+} doped $\text{TeO}_2\text{--WO}_3$ glass. *Spectrochim. Acta A*, 2001, **57**, 2367–2372.
20. Özen, G., Demirata, B. and Öveçoğlu, M. L., Effect of composition on the thermal properties and spontaneous emission probabilities of Tm^{3+} doped $\text{TeO}_2\text{--LiCl}$ glass. *J. Mater. Res.*, 2001, **16**, 1381–1388.
21. Eşin, C., Kabalcı, İ., Öveçoğlu, M. L. and Özen, G., Crystallization behavior of $(1-x)\text{TeO}_2\text{--}x\text{BaO}$ ($x=0.10, 0.15$ and 0.25 in molar ratio) glasses. *J. Eur. Ceram. Soc.*, 2007, **27**(2–3), 1797–1800.
22. Öveçoğlu, M. L., Özen, G., Demirata, B. and Genç, A., Microstructural characterization and crystallization kinetics of $(1-x)\text{TeO}_2\text{--}x\text{LiCl}$ ($x=0.6\text{--}0.4$ mol) glasses. *J. Eur. Ceram. Soc.*, 2007, **27**, 1823–1827.
23. Weil, M., New phases in the systems Ca--Te--O and Cd--Te--O : the calcium tellurite(IV) $\text{Ca}_4\text{Te}_5\text{O}_{14}$, and the cadmium compounds $\text{Cd}_2\text{Te}_3\text{O}_9$ and $\text{Cd}_2\text{Te}_2\text{O}_7$ with mixed-valent oxotellurium(IV/VI) anions. *Solid State Sciences*, 2004, **6**, 29–37.
24. Öveçoğlu, M. L., Özen, G. and Cenk, S., Microstructural characterization and crystallization behavior of $(1-x)\text{TeO}_2\text{--}x\text{WO}_3$ ($x=0.15, 0.25, 0.3$ mol) glasses. *J. Eur. Ceram. Soc.*, 2006, **26**(7), 1149–1158.
25. Ruvalcaba-Cornejo, C., Flores-Acosta, M., Elena Zayas, Ma., Lozada-Morales, R., Palomino-Merino, R., Espinosa, J. E. et al., Photo luminescence properties of the ZnO--CdO--TeO_2 system doped with the Tb^{3+} and Yb^{3+} ions. *J. Lumin.*, 2008, **128**(2), 213–216.
26. Dodd, J. W. and Tonge, K. H., *Thermal Methods*. John Wiley & Sons, London, 1987.
27. Powder Diffraction Files: Card No. 42-1365, Database Edition, The International Centre for Diffraction Data (ICDD).
28. Powder Diffraction Files: Card No. 52-0795, Database Edition, The International Centre for Diffraction Data (ICDD).
29. Powder Diffraction Files: Card No. 49-1745, Database Edition, The International Centre for Diffraction Data (ICDD).
30. Powder Diffraction Files: Card No. 36-0345, Database Edition, The International Centre for Diffraction Data (ICDD).